amb@iaa.es

# The ALHAMBRA-survey:

## Bayesian Photometric Redshifts for 3 deg$^2$

A. Molino, N. Benítez, M. Moles + the ALHAMBRA collaboration.

## Introduction

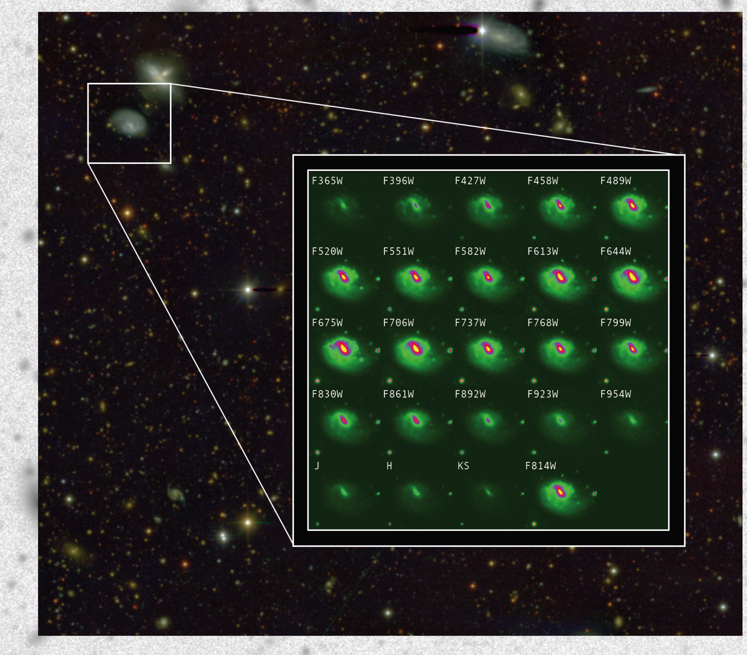

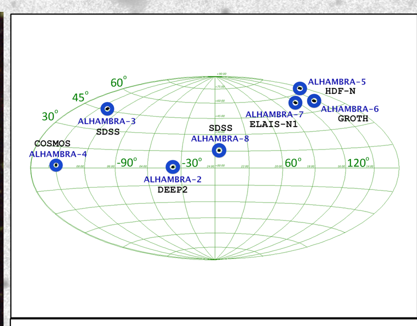

| Field Name | Overlapping Survey | RA (J2000) | DEC (J2000) | Area / Effective [deg$^2$] | Number catalogs | Science Images | Detected Sources | Density (*) [#/deg$^2$] |
|---|---|---|---|---|---|---|---|---|
| ALHAMBRA-1 | — | 00 29 46.0 | +05 25 30 | 0.50 / — | — | 192 | — | — |
| ALHAMBRA-2 | DEEP2 | 01 30 16.0 | +04 15 40 | 0.50 / 0.45 | 8 | 192 | 67.791 | 77.144 |
| ALHAMBRA-3 | SDSS | 09 16 20.0 | +46 02 20 | 0.50 / 0.47 | 8 | 192 | 68.015 | 75.000 |
| ALHAMBRA-4 | COSMOS | 10 00 00.0 | +02 05 11 | 0.25 / 0.23 | 4 | 96 | 38.464 | 93.261 |
| ALHAMBRA-5 | HDF-N | 12 35 00.0 | +61 57 00 | 0.25 / 0.24 | 4 | 96 | 42.618 | 82.300 |
| ALHAMBRA-6 | GROTH | 14 16 38.0 | +52 24 50 | 0.50 / 0.47 | 8 | 192 | 66.906 | 77.740 |
| ALHAMBRA-7 | ELAIS-N1 | 16 12 10.0 | +54 30 15 | 0.50 / 0.47 | 8 | 192 | 79.453 | 82.185 |
| ALHAMBRA-8 | SDSS | 23 45 50.0 | +15 35 05 | 0.50 / 0.46 | 8 | 192 | 75.109 | 82.452 |
| | | | | 3.50 / 2.79 | 48 | 1344 | 438.356 | <81.440> |

* F814W < 24.

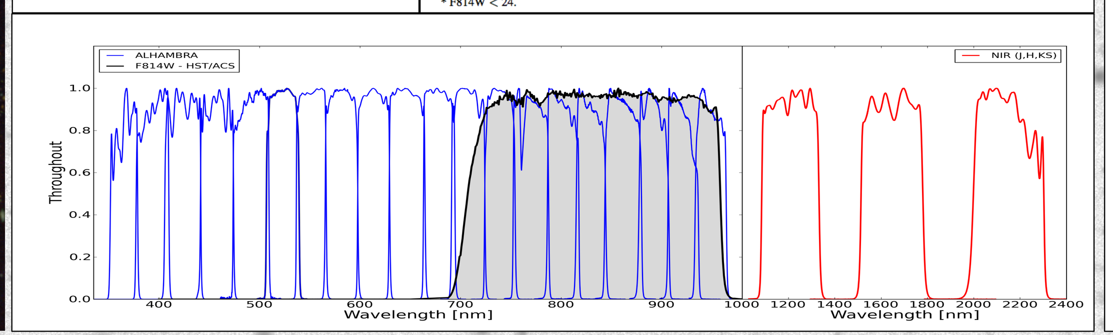


| CAMERA | FILTER | $\lambda_{eff}$ [Å] | FWHM [Å] | $\langle t_{exp} \rangle$ [sec] | $\langle m_{lim}^{(3")} \rangle$ (5-$\sigma$) |
|---|---|---|---|---|---|
| Optical | | | | | |
| LAICA | F365W | 365 | 279 | 3918 | 23.7 |
| LAICA | F396W | 396 | 330 | 2896 | 23.8 |
| LAICA | F427W | 427 | 342 | 2774 | 23.8 |
| LAICA | F458W | 458 | 332 | 3079 | 23.8 |
| LAICA | F489W | 489 | 356 | 2904 | 24.2 |
| LAICA | F520W | 520 | 326 | 2664 | 24.1 |
| LAICA | F551W | 551 | 297 | 2687 | 23.7 |
| LAICA | F582W | 582 | 324 | 2936 | 23.8 |
| LAICA | F613W | 613 | 320 | 2940 | 23.9 |
| LAICA | F644W | 644 | 357 | 4043 | 23.8 |
| LAICA | F675W | 675 | 314 | 4575 | 23.5 |
| LAICA | F706W | 706 | 332 | 5668 | 23.7 |
| LAICA | F737W | 737 | 304 | 7095 | 23.5 |
| LAICA | F768W | 768 | 354 | 8824 | 23.5 |
| LAICA | F799W | 799 | 312 | 8992 | 23.2 |
| LAICA | F830W | 830 | 296 | 11436 | 23.2 |
| LAICA | F861W | 861 | 369 | 10505 | 22.9 |
| LAICA | F892W | 892 | 303 | 9044 | 22.5 |
| LAICA | F923W | 923 | 308 | 6338 | 22.1 |
| LAICA | F954W | 954 | 319 | 5620 | 21.5 |
| NIR | | | | | |
| OMEGA | $H$ | 1216 | 2163 | 5169 | 22.6 |
| OMEGA | $J$ | 1655 | 2191 | 5055 | 21.9 |
| OMEGA | $Ks$ | 2146 | 2412 | 5050 | 21.4 |
| Detection | | | | | |
| SYNTH | F814W | 845 | 2366 | 73522 | 24.5 |

The **ALHAMBRA** (**A**dvance **L**arge **H**omogeneous **A**rea **M**edium **B**and **R**edshift **A**stronomical) survey (Moles et al. 2008) has imaged a total area of 3.5 deg2 among eight separated regions of the sky, including sections of the COSMOS, DEEP2, ELAIS, GOODS-N, SDSS and Groth fields. Observations have been carried out on the 3.5m telescope on the Calar Alto Observatory (CAHA, Spain) making use of the two wide-field imagers in the optical (LAICA) and in the NIR (Omega-2000), up to reach a total on-target integration time of ~27.8hrs for medium-band filters and ~4.2hrs for broadband Near Infrared (NIR) filters. The photometric system, covering the whole optical range (3500Å to 9700Å) with 20 contiguous, equal-width, non overlapping, medium-band filters along with the standard JHKs NIR bands, has been specifically designed to optimize photometric redshift depth and accuracy (Benítez et al. 2009b, Aparicio-Villegas et al. 2010), while keeping the capability of detecting and identifying relatively faint emission lines (Bongiovanni et al. 2010, Matute et al. 2012).

## Synthetic F814W images

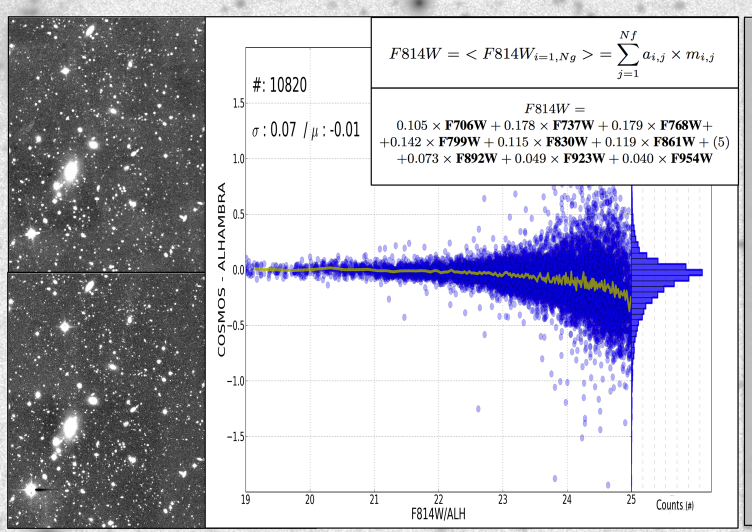


To define a constant and homogeneous window for all ALHAMBRA fields, we generated synthetic F814W images as the combination of individual bands. To properly calculate the color transformations we used a population of galaxies with typical z, magnitude and spectral-type and solved the system of equations generated when estimating the correspondence between sythetic magnitudes among the different filters. To verify the calibration of the synthetic F814W images, we performed a photometric comparison with the COSMOS field. To reproduce the same photometric measurements as in (Ilbert et al. 2009), we ran SExtractor using fixed circular apertures of 3". We retrieved ~10800 common sources with ALHAMBRA compresing magnitudes from 19<F814W<25.5. Photometric zp offsets or trends with magn. down to F814W<23.5 were not observed.

## PSF-Photometry

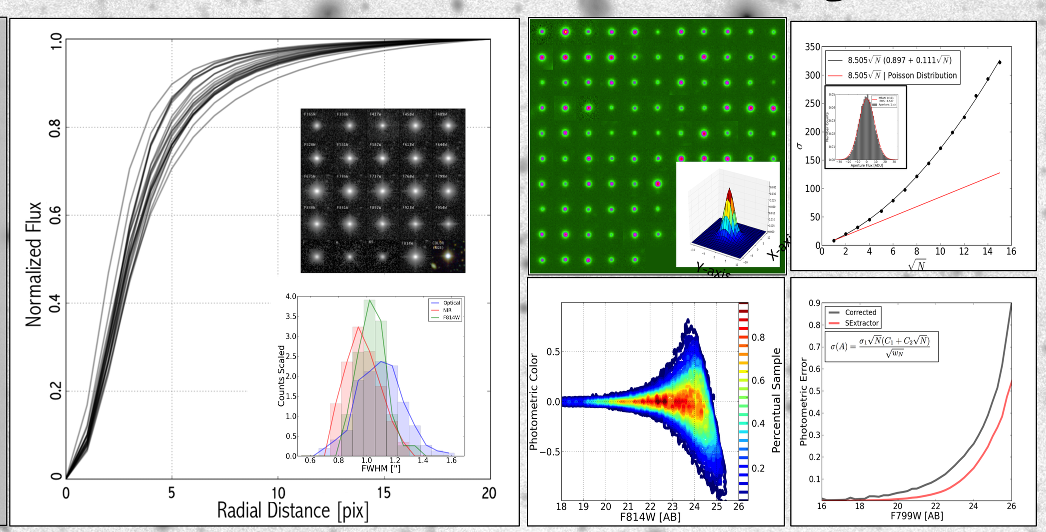


To perform good quality multi-color photometry, it is necesary o sample the same region of the galaxy and to take into account the smearing produced by different PSFs. The distribution of PSFs in the ALHAMBRA survey compresses values from 0.7" to 1.6". We relied on *ColorPro* (Coe et al. 2006) to derive accurate PSF-corrected photometry without degrading high quality images. PSF-models were carefully generated for every image. We designed a set of simulations to test the accuracy of *ColorPro* retrieving precise photometry across images with varied PSF. We found a dispersion below of 3% for magnitudes brighter than F814W=23.0, and 5% for F814W=24.5

## Bayesian Photometric Redshifts

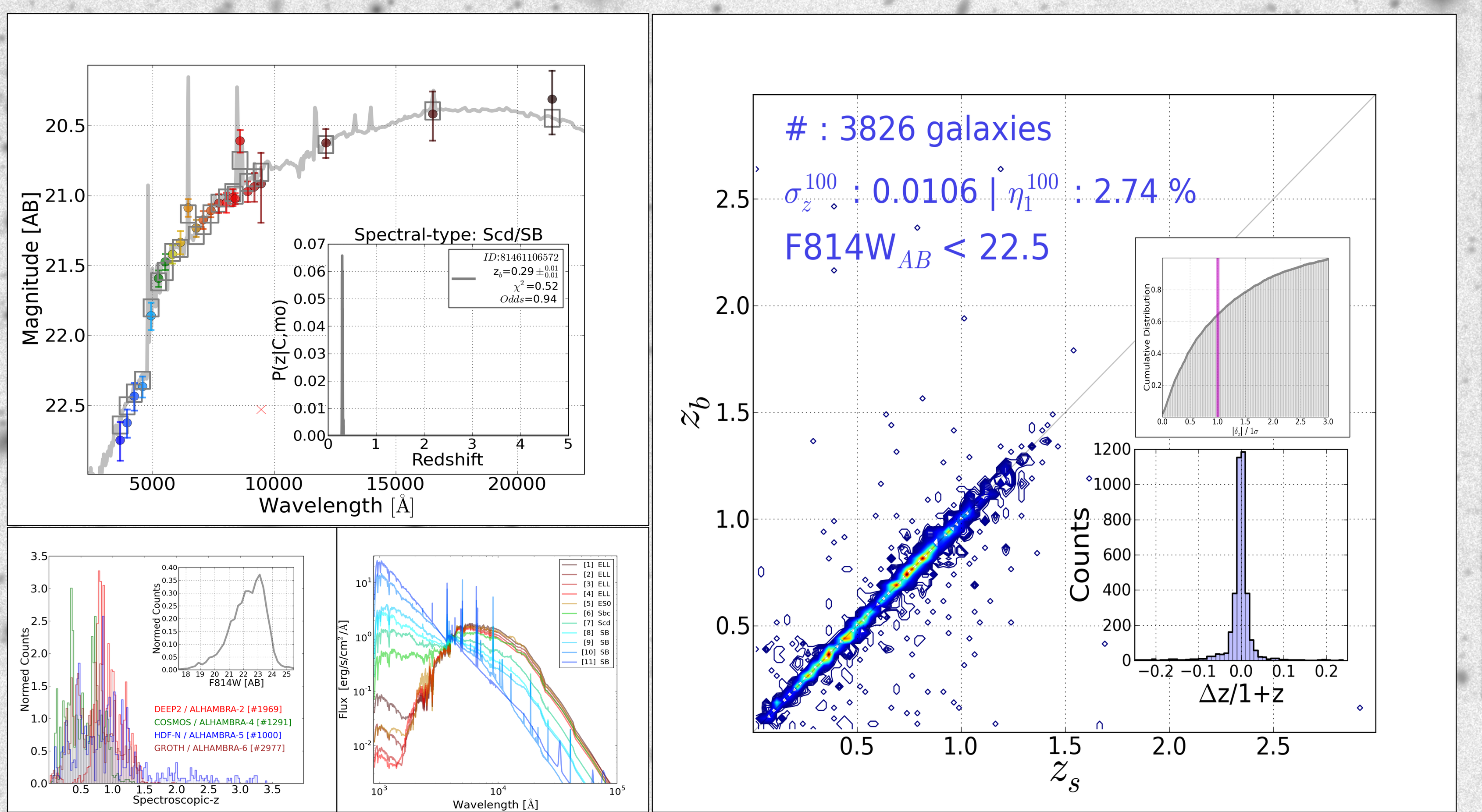


BPZ (Benítez 2000) is a SED-fitting method optimized to compute accurate photometric redshifts. Unlike most similar codes, BPZ in- troduces the use of a Bayesian inference where a maximum like- lihood (resulting from a χ2 minimization between the observed and predicted colors for a galaxy, among a range of redshifts and templates) is weighted by a prior probability. We used a new prior of BPZ (Benítez 2013, in prep.) which gives the probability of a galaxy with apparent magnitude m0 of having a certain redshift z and spectral-type T , empirically derived for each spectral-type and magnitude by fitting luminosity functions provided by GOODS- MUSIC (Santini et al. 2009), COSMOS (Scoville et al. 2007) and UDF (Coe et al.2006). As the resulting p(z,T) is usually a multimodal distribution (with more than one possible peak given the color-redshift degeracies) the inclusion of any prior information in the analysis serves to eliminate unrealistic solutions reducing the number of catastrophic outliers. BPZ uses a new library (Benítez 2013) composed by five SED templates originally drawn from PEGASE (Fioc & Rocca- Volmerange 1997) but then re-calibrated using the FIREWORKS photometry and spectroscopic redshifts (Wuyts et al. 2008) to opti- mize its performance, i.e., making the templates to have same col- ors as real galaxies with known redshifts observed with ACS. In ad- dition five GRASIL and one Starburst templates have been added. This new library includes five templates for elliptical galaxies, two for spiral galaxies and four for starburst galaxies along with emission lines and dust extinction. The opacity of the intergalactic medium was applied as described in Madau et al. (1995). An example of the typical spectral-fitting using the ALHAMBRA photometry is shown in the figure.

In this work, we present photometric redshifts for ~**440,000 galaxies**. When compared with a sample of ~7000 galaxies with spectroscopic redshifts, our photometric redshifts have a precision of **δz/(1+zs)=1%** for I<22.5 and **δz/(1+zs)=1.4%** for **22.5<I<24.5**. Precisions of **δz /(1+zs)< 0.5%** are reached for about 30% of the spectroscopic sample, showing the potential of medium-band photometric surveys.

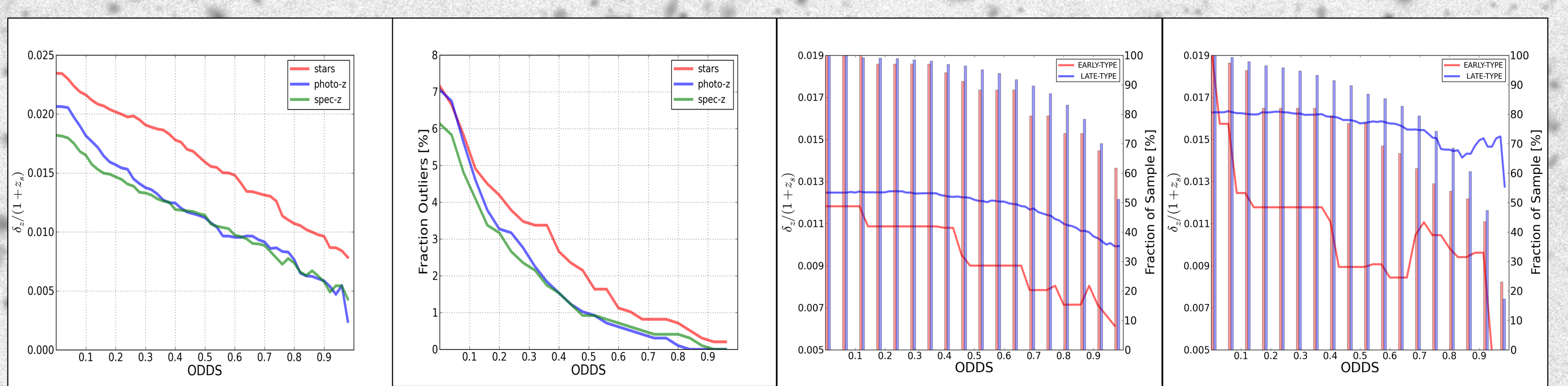


## Zeropoint auto-calibration

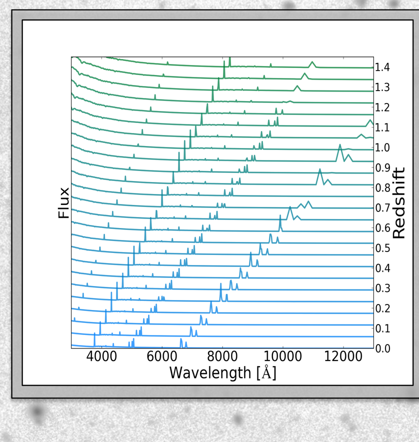


We realized that the photometric redshifts obtained for emission line galaxies were quite robust to changes in the zeropoint calibration and therefore we could treat those redshifts as spectroscopic for calibration purposes, obtaining an automatic and self-contained zeropoint correction for all our fields. Figures show the photometric redshift accuracy when using three different calibration methods: the original zeropoints (red line), corrections derived from photo-z (blue line) and corrections from spectroscopic redshifts (green line). The results indicate that the methodology presented here successfully improved the photometric redshifts accuracy al-sample, and it also dramatically reduces the fraction of catastrophic outliers

## Redshift Probability Distribution Function & the Cosmic Variance

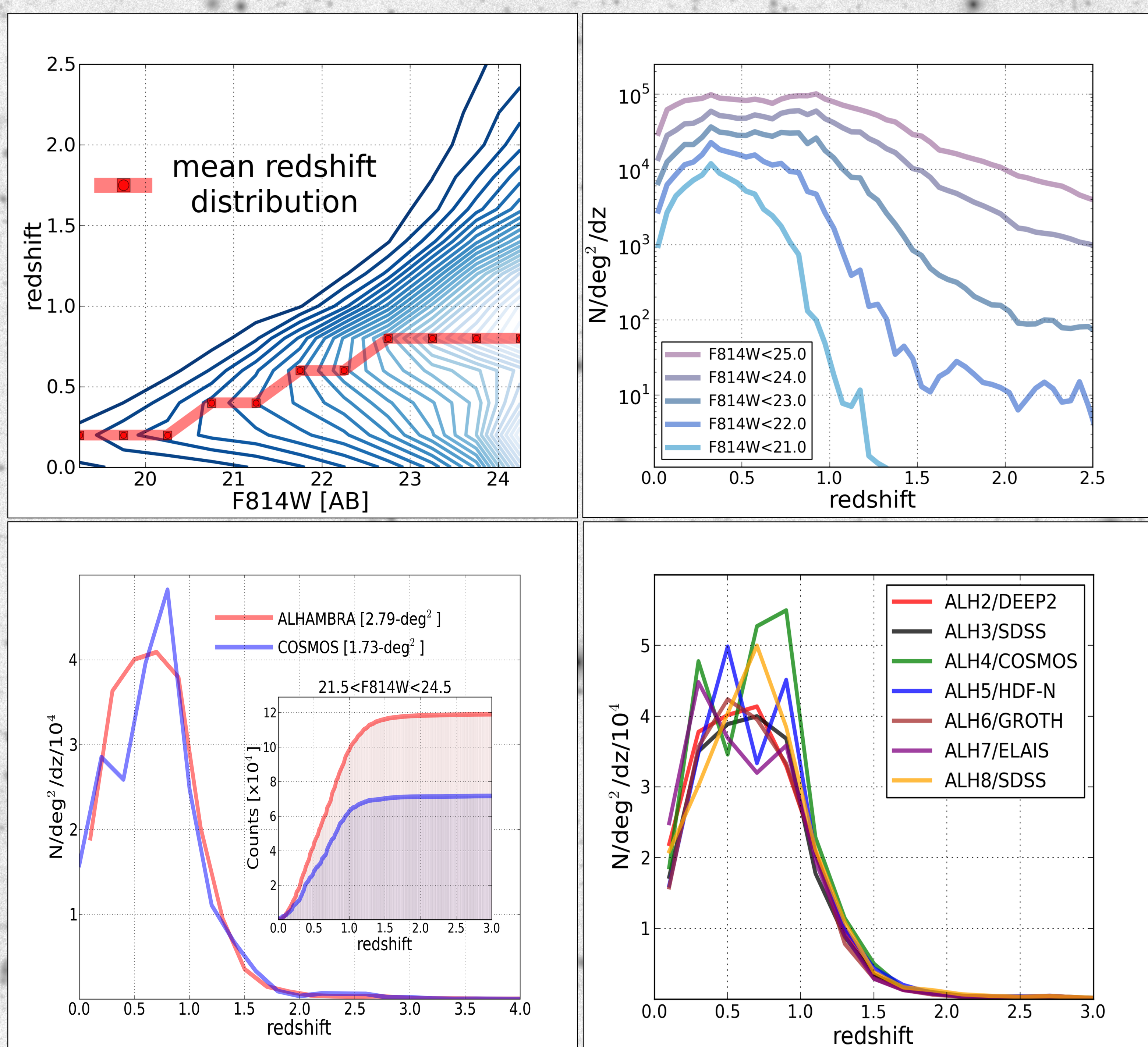


Considering the probabilistic nature of the photometric redshift estimations, instead of relying on the most likely solution (given by any point estimate) it is desirable to make use of the complete information yielded by the Probab. Distrib. Functions *P(z, T|C)*

$$P(z) = \sum_{i=1}^{N_g} P_i(z) = \sum_{i=1}^{N_g} \left[ \frac{\int dT\, p_i(z,T)}{\int dT \int dz p_i(z,T)} \right]$$

In order to study the cosmic variance across the fields and compare it with other surveys,we ran BPZ on the photometric catalogue used by Ilbert et al. (2009) to derive the global redshift probability distribution function P(z) for the COSMOS field. We initially compared the P(z) derived using the ALHAMBRA-4 data (red line) with the P (z) derived us- ing the COSMOS data (blue line), where both distributions consistently reproduce a double peak at redshifts z~0.3 and z~0.9, respectively. However, whereas the ALHAMBRA-4 field shows a mean redshift ⟨z⟩ = 0.60 for F814W < 22.5 and ⟨z⟩ = 0.87 for F814W < 25.5, the COSMOS field shows a mean redshift ⟨z⟩ = 0.66 for F814W < 22.5 and ⟨z⟩ = 0.96 for F814W<25.5. Meanwhile the global photometric redshift distribution derived for all the seven ALHAMBRA fields (excluding stars) shows a mean redshift ⟨z⟩ = 0.56 for F814W<22.5 and ⟨z⟩ = 0.85 for F814W < 25.5. This result indicates that the COSMOS field shows a clear over-density with respect to the mean value de- rived averaging the seven ALHAMBRA fields. In fact, the average galaxy number in COSMOS goes up by a 60% between z=0.4 and z=0.7, whereas no such effect is observed in our average.

We derived the averaged redshift probability distribution function for the ALHAMBRA fields, to study its evolution as a function of the magnitude F814W and redshift. The solid red line corresponding to the ⟨z⟩ distribution (per bins of 0.5 mags) indicates a clear evolution effect moving from a ⟨z⟩~0.2 for F814W<20.5 to a ⟨z⟩~0.8 for F814W>23.0. Inversely, the peak of the averaged distribution of galaxies increases as a function of the z for different ranges in magnitude.